Plant Sci. Arc.
Plant Science Archives
An International Journal of Plant Biology

Original Research Article
ISSN 2518-6965
Journal Homepage: www.plantarc.com

Evaluation of the Anti-Hyperglycemic Potential of *Basella alba* and Its Zinc Oxide Nanoparticles

Swathi Badabagni[1], Palempalli Uma Maheswari Devi*[1], O Vijaya Sarathi Reddy[2], and Balaji Meriga[2]

[1]*Department of Applied Microbiology, Sri Padmavati Mahila Visvavidyalayam, Padmavathi Nagar, Tirupati, Andhra Pradesh 517502, India*
[2]*Department of Biochemistry, Sri Venkateswara University, Tirupati, Andhra Pradesh 517502, India*

Citation: Swathi Badabagni, Palempalli Uma Maheswari Devi, O Vijaya Sarathi Reddy, and Balaji Meriga (2026). Evaluation of the Anti-Hyperglycemic Potential of *Basella alba* and Its Zinc Oxide Nanoparticles. *Plant Science Archives.*
DOI: https://doi.org/10.51470/PSA.2026.11.3.123

Corresponding Author: **P. Uma Maheswari Devi** | E-Mail: **(umadevi66@gmail.com)**

Received 11 June 2026 | Revised 09 July 2026 | Accepted 14 August 2026 | Available Online 13 September 2026

ABSTRACT

Basella alba is a nutritionally important leafy vegetable with considerable potential as a source of bioactive phytochemicals. This study investigated the phytomediated synthesis of zinc oxide nanoparticles (BA-ZnONPs) using B. alba leaf extract and comparatively evaluated their in vitro and in vivo antihyperglycemic activities against the aqueous extract of B. alba (BAAE). The synthesized nanoparticles were characterized using UV–visible spectroscopy, Fourier-transform infrared spectroscopy (FTIR), X-ray diffraction (XRD), dynamic light scattering (DLS), zeta potential analysis, scanning electron microscopy (SEM), energy-dispersive X-ray spectroscopy (EDX), and atomic force microscopy (AFM). The characterization results supported the formation of crystalline ZnO nanoparticles with a reported hydrodynamic size of 1.4 nm, a zeta potential of −38.2 mV, and a hexagonal wurtzite crystal structure. EDX analysis revealed zinc and oxygen contents of 44.87% and 55.13%, respectively. In vitro enzyme inhibition assays demonstrated that BA-ZnONPs inhibited α-amylase and α-glucosidase activities, with greater inhibitory activity than BAAE and the reference inhibitor acarbose. The α-glucosidase inhibitory activity of BA-ZnONPs was particularly pronounced, with an IC_{50} value of 43.34 µg/mL compared with 90.14 µg/mL for acarbose. In streptozotocin (STZ)-induced diabetic rats, oral administration of BA-ZnONPs (50 mg/kg body weight) produced a 79.07% reduction in fasting blood glucose after 42 days, whereas BAAE (500 mg/kg body weight) produced a 75.78% reduction. BA-ZnONPs treatment also improved glucose tolerance, restored hepatic and muscle glycogen levels, modulated the activities of carbohydrate-metabolizing enzymes, and improved body weight relative to the diabetic control. Histopathological examination further revealed substantial preservation and restoration of pancreatic islet architecture, accompanied by an apparent improvement in β-cell integrity. BA-ZnONPs exhibited enhanced antihyperglycemic activity compared with the crude aqueous extract at substantially lower doses. These findings suggest that B. alba-mediated ZnO nanoparticles represent a promising plant-based nanomaterial for further investigation in diabetes-related research, although detailed mechanistic and toxicological studies are required to establish their therapeutic potential.

Keywords: *Basella alba, Phytomediated Synthesis, Zinc Oxide Nanoparticles, α-amylase and α-glucosidase, STZ models.*

Graphical Abstract

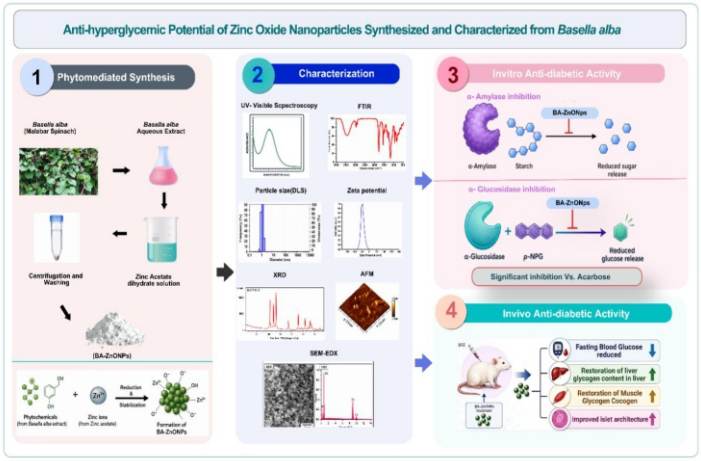

1. Introduction

Diabetes mellitus (DM) is a chronic metabolic disorder characterized by persistent hyperglycemia arising from impaired insulin secretion, reduced insulin sensitivity, or a combination of both mechanisms [1]. The disease is associated with progressive dysfunction of multiple organs and represents a major risk factor for several long-term complications, particularly those affecting the nervous system, kidneys, liver, and cardiovascular system [2]. Sustained hyperglycemia promotes the excessive generation of reactive oxygen species (ROS), resulting in oxidative stress, cellular damage, and impaired pancreatic β-cell function [3]. In addition to disturbances in glucose and insulin metabolism, alterations in trace-element homeostasis may further contribute to the pathophysiology of diabetes. Zinc, in particular, plays an essential role in insulin biosynthesis, storage, secretion, and biological activity, thereby contributing to the maintenance of normal glucose homeostasis [4,5].

Although several pharmacological approaches are currently available for glycemic management, their long-term use may be constrained by adverse effects, treatment costs, and variable therapeutic responses [6]. Consequently, considerable research interest has focused on plant-derived bioactive compounds as potential complementary sources of antidiabetic agents. Medicinal plants contain diverse phytochemical constituents, including flavonoids, phenolic compounds, tannins, alkaloids, and sterols, which may influence glucose metabolism through multiple mechanisms. These include the inhibition of carbohydrate-hydrolyzing enzymes, particularly α-amylase and α-glucosidase, as well as the modulation of oxidative stress and insulin-associated signalling pathways. The identification and evaluation of such plant-derived compounds may therefore contribute to the development of alternative strategies for improving glycemic control.

Basella alba L. (family *Basellaceae*), commonly known as Malabar spinach, has attracted attention because of its phytochemical composition and reported therapeutic properties [7,8]. Despite its nutritional and medicinal significance, investigations into the potential antidiabetic applications of *B. alba* have largely focused on crude plant extracts [9]. Conventional extracts, however, may present limitations associated with the stability, solubility, bioavailability, and effective delivery of their constituent phytochemicals. Recent developments in green nanotechnology offer an alternative approach to addressing some of these limitations by employing plant extracts as reducing, stabilizing, or capping agents during nanoparticle synthesis. Such plant-mediated synthesis also provides an opportunity to investigate the combined functional properties of plant-derived constituents and inorganic nanomaterials. Among metal oxide nanomaterials, zinc oxide nanoparticles (ZnONPs) have received considerable attention because of their physicochemical properties, including high surface-area-to-volume ratio, catalytic activity, and potential biological applications [10–15]. Their interaction with biological systems may influence cellular and metabolic processes relevant to glucose regulation. Furthermore, ZnO has been recognized by the United States Food and Drug Administration as a substance generally recognized as safe (GRAS) for specified applications [16]. However, this designation should not be interpreted as establishing the safety of all ZnONPs formulations, since their biological effects may vary depending on particle size, surface characteristics, concentration, route of exposure, and duration of treatment. Therefore, the biological activity and safety of plant-mediated ZnONPs require systematic experimental evaluation.

Considering the biological significance of zinc and the phytochemical potential of *B. alba*, the present study investigated the green synthesis of zinc oxide nanoparticles using *B. alba* leaf extract and evaluated their potential antihyperglycemic activity. The synthesized *B. alba*-mediated zinc oxide nanoparticles (BA-ZnONPs) were characterized using complementary physicochemical and morphological techniques. Their biological activity was subsequently assessed through *in vitro* inhibition of carbohydrate-hydrolyzing enzymes and glucose-regulation studies in an experimental model of diabetes. By comparing the activities of BA-ZnONPs with those of the corresponding aqueous plant extract, this study aimed to determine whether plant-mediated ZnO nanoparticle synthesis could improve the observed antidiabetic potential of *B. alba*.

The findings are expected to provide an experimental basis for further investigation of plant-derived ZnO nanomaterials as potential candidates for diabetes-related research.

2. Materials and Methods

2.1. Phytomediated Synthesis and Characterization of BA-ZnONPs

Basella alba L. leaves were collected from authenticated local sources in Tirupati, India, and taxonomically identified. A voucher specimen was deposited under accession number SVUTY-01797. The collected leaves were washed, dried, and powdered. For aqueous extraction, 10 g of powdered leaf material was mixed with 100 mL of Milli-Q water and heated at 80 °C for 30 min. The resulting extract was used for the phytomediated synthesis of zinc oxide nanoparticles. For nanoparticle synthesis, 0.02 M zinc acetate dihydrate was mixed with 10 mL of *B. alba* leaf extract. The reaction mixture was stirred at room temperature for 10 min under alkaline conditions (pH 12). The mixture was maintained under stirring conditions for 2 hours at room temperature to facilitate the formation of zinc oxide nanoparticles, as indicated by a distinct colour change from pale yellow to milky white. The resulting suspension was centrifuged at 10,000 rpm for 15 min, and the collected precipitate was washed three times with distilled water, followed by ethanol, to remove residual ions and other impurities [17]. The purified precipitate was subsequently dried at 80 °C to obtain the phytomediated zinc oxide nanoparticle powder, designated BA-ZnONPs.

The synthesized BA-ZnONPs were characterized using complementary analytical techniques to evaluate their optical, structural, physicochemical, morphological, and elemental properties. UV–visible spectroscopy was used to examine the characteristic optical absorption profile associated with nanoparticle formation. Fourier-transform infrared (FTIR) spectroscopy was performed to identify the functional groups present in the *B. alba* aqueous extract (BAAE) and BA-ZnONPs and to investigate the possible involvement of plant-derived phytochemicals in nanoparticle formation and surface stabilization. X-ray diffraction (XRD) analysis was conducted to determine the crystalline structure and phase characteristics of the synthesized nanoparticles. Dynamic light scattering (DLS) was used to determine the hydrodynamic particle-size distribution, while zeta potential measurements were performed to assess the surface charge characteristics and colloidal stability. Scanning electron microscopy (SEM) coupled with energy-dispersive X-ray spectroscopy (EDX/EDAX) was employed to examine the surface morphology and elemental composition. In addition, atomic force microscopy (AFM) was used to evaluate the surface topography and three-dimensional morphological characteristics of BA-ZnONPs.

2.2. *In Vitro* Antidiabetic Assays

2.2.1. α-Amylase and α-glucosidase inhibitory assays

The α-amylase inhibitory activity of BA-ZnONPs was evaluated at concentrations ranging from 20 to 100 µg/mL using the dinitrosalicylic acid (DNS) method, with starch as the substrate [18]. Following the enzymatic reaction, the reducing sugars released from starch hydrolysis were quantified using the DNS reagent, and absorbance was measured at 540 nm. The inhibitory activity was calculated relative to the corresponding control. The α-glucosidase inhibitory activity was determined using *p*-nitrophenyl-α-D-glucopyranoside as the substrate, with acarbose serving as the positive control [19].

The extent of enzyme inhibition was evaluated based on the reduction in the formation of the reaction product relative to the control.

2.3. *In Vivo* Assessment of the Antihyperglycemic Potential of BA-ZnONPs

2.3.1. Experimental Animals and Acute Toxicity Analysis

Male Wistar albino rats weighing 160–240 g were used for the animal experiments. The animals were maintained under standard experimental conditions, and all procedures were performed in accordance with the guidelines of the Committee for Control and Supervision of Experiments on Animals (CPCSEA), following approval from the Institutional Animal Ethics Committee (IAEC approval number: CPCSEA/1677/PO/Re/S/2012/IAEC/07). The acute toxicity profiles of BAAE and BA-ZnONPs were evaluated at doses of 1,000 and 2,000 mg/kg body weight and 500 and 1,000 mg/kg body weight, respectively, with six animals assigned to each group. The assessments were conducted according to OECD Test Guidelines 423 and 425, respectively [20]. Animals were monitored for clinical signs of toxicity and mortality during the initial 24 h and subsequently at regular intervals over a 14-day observation period.

2.3.2. Short-Term Effects of BAAE and BA-ZnONPs on Oral Glucose Tolerance

Experimental diabetes was induced by a single intraperitoneal injection of streptozotocin (STZ), following the method standardized in our laboratory [21]. To prevent acute hypoglycemia following STZ administration, the rats were provided with a 5% glucose solution 6 h after injection. After 72 h, fasting blood glucose levels were measured, and animals with glucose concentrations exceeding 200 mg/dL were considered diabetic. Control animals received an equivalent volume of saline [22]. The short-term antihyperglycemic effects of BAAE (250 and 500 mg/kg body weight) and BA-ZnONPs (25 and 50 mg/kg body weight) were evaluated by monitoring blood glucose levels at predetermined intervals over a 6-h period following treatment. To assess glucose tolerance, the animals were orally administered a glucose load of 2 g/kg body weight, and subsequent changes in blood glucose levels were recorded. The responses to BAAE and BA-ZnONPs were evaluated in STZ-induced diabetic rats.

2.3.3. Long-Term Antidiabetic Study

The long-term antihyperglycemic effects of BAAE (250 and 500 mg/kg body weight) and BA-ZnONPs (25 and 50 mg/kg body weight) were investigated in STZ-induced diabetic rats over a 42-day experimental period. Changes in body weight and fasting blood glucose levels were monitored throughout the study. Glibenclamide (25 mg/kg body weight) was included as the reference antidiabetic treatment for comparison. At the end of the experimental period, the animals were euthanized, and liver and pancreatic tissues were collected for subsequent biochemical and histopathological analyses.

2.3.4. Effects of BAAE and BA-ZnONPs on Carbohydrate-Metabolizing Enzymes

The activities of selected carbohydrate-metabolizing enzymes were evaluated in tissue samples following the respective assay procedures.

For the hexokinase assay, liver or kidney tissue homogenates were incubated at 37 °C in a reaction mixture containing glucose, ATP, $MgCl_2$, NaF, KH_2PO_4, and KCl. Enzyme activity was expressed as µmol of glucose phosphorylated per hour per milligram of protein (µmol/h/mg protein) [25]. Glucose-6-phosphate dehydrogenase (G6PDH) activity was determined by monitoring the reduction of $NADP^+$ to NADPH at 340 nm. The enzyme activity was expressed as units per minute per milligram of protein (U/min/mg protein) [26]. Hepatic glucose-6-phosphatase and fructose-1,6-bisphosphatase activities were determined by measuring the amount of inorganic phosphate liberated during the respective enzymatic reactions. Absorbance was recorded at 620 nm, and enzyme activities were expressed as µmol of inorganic phosphate liberated per minute per milligram of protein (µmol/min/mg protein) [27].

2.3.5. Effects of BAAE and BA-ZnONPs on Hepatic Glucose and Glycogen levels

Hepatic glucose content was estimated using a standard glucose calibration curve, and the results were expressed as milligrams per gram of wet tissue (mg/g tissue) [23,24]. Hepatic and skeletal muscle glycogen contents were quantitatively determined using the anthrone method [29]. Briefly, 250 mg of tissue was homogenized in 30% KOH, and glycogen was precipitated using saturated sodium sulfate and ethanol. The resulting glycogen pellet was treated with anthrone reagent, and absorbance was measured at 660 nm. Glycogen content was calculated and expressed as milligrams per 100 g of tissue (mg/g tissue).

2.3.6. Histopathological Analysis

Pancreatic tissues collected at the end of the experimental period were fixed in 10% formalin, processed using standard histological procedures, and embedded for sectioning. Thin sections of approximately 5 µm thickness were prepared and stained with hematoxylin and eosin (H&E). The stained sections were mounted using DPX mounting medium and examined microscopically to evaluate histopathological alterations in pancreatic tissue architecture.

2.4. Statistical Analysis

All experiments were conducted in triplicate (n = 3) and with six animals per group (n = 6) for *in vitro* and *in vivo* analysis, respectively. Statistical analysis was performed using one-way ANOVA to assess intergroup differences, and nonlinear regression analysis using GraphPad Prism software (version 9.1.2) was adopted for obtaining IC50 Values.

3. Results

3.1. Green Synthesis and Physicochemical Characterization of BA-ZnONPs

The aqueous leaf extract of *Basella alba* successfully facilitated the phytomediated synthesis of zinc oxide nanoparticles (BA-ZnONPs). A visible colour change was observed during the synthesis process, indicating the formation of the nanoparticle suspension. UV–visible spectroscopic analysis revealed a broad, low-intensity absorption band between 200 and 400 nm in the *B. alba* aqueous extract (BAAE) (Fig. 1A). In contrast, the BA-ZnONPs exhibited a distinct absorption maximum at 372 nm, consistent with the characteristic optical absorption reported for ZnO nanomaterials. The differences between the absorption profiles of BAAE and BA-ZnONPs indicate changes in the optical properties following nanoparticle synthesis.

FTIR analysis revealed prominent absorption bands at 1660.16 cm^{-1}, which were assigned to C=O/C=C stretching vibrations associated with carbonyl and aromatic groups. Additional bands at 1382.36 and 1324.86 cm^{-1} were attributed to C–O stretching vibrations of carboxyl- and phenolic-group-containing compounds. Several characteristic bands observed in BAAE exhibited shifts or changes in intensity following nanoparticle synthesis, suggesting the involvement of plant-derived functional groups in the formation and surface stabilization of BA-ZnONPs. The absorption bands at 450.58 and 416.33 cm^{-1} were assigned to metal–oxygen vibrations, supporting the formation of ZnO (Fig. 1B).

Dynamic light scattering analysis indicated a reported particle size of 1.4 nm (Fig. 1C), while the zeta potential was −38.2 mV (Fig. 1D), indicating a negatively charged particle surface and suggesting favourable electrostatic stabilization under the measurement conditions. X-ray diffraction analysis revealed distinct diffraction peaks at 2θ values of approximately 31.74°, 34.38°, 36.21°, 47.43°, 56.55°, 62.79°, 66.40°, 67.94°, 68.96°, 72.49°, and 76.92°. These reflections corresponded to the (100), (002), (101), (102), (110), (103), (200), (112), (201), (004), and (202) crystallographic planes, respectively. The diffraction pattern was consistent with the hexagonal wurtzite structure of ZnO (JCPDS card no. 36-1451), confirming the crystalline nature of the synthesized material (Fig. 1E).

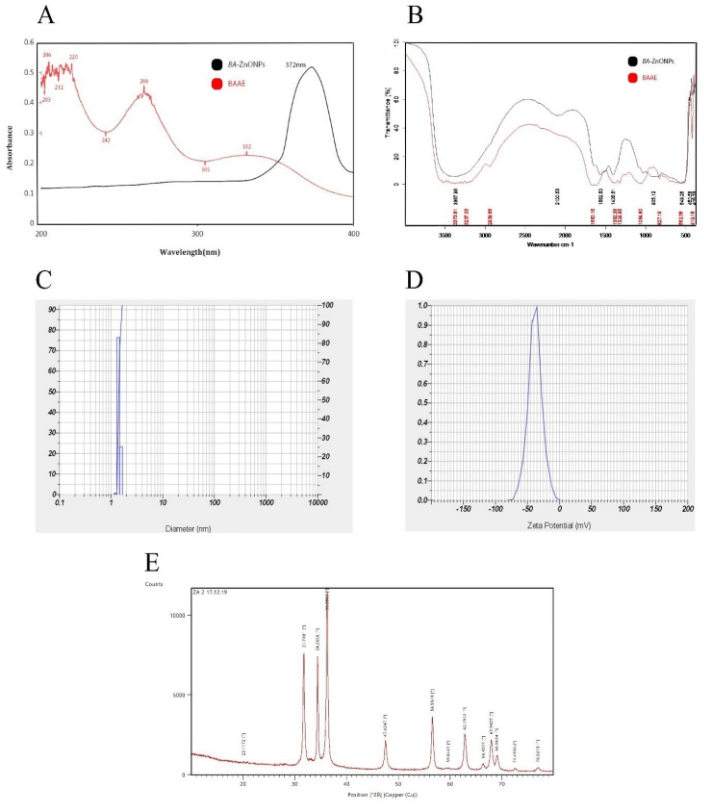

Fig. 1. Physicochemical characterization of zinc oxide nanoparticles synthesized using *Basella alba* leaf extract (BA-ZnONPs). (A) UV–visible absorption spectra of BAAE and BA-ZnONPs; (B) Fourier-transform infrared (FTIR) spectra of BAAE and BA-ZnONPs; (C) particle-size distribution profile of BA-ZnONPs; (D) zeta potential distribution of BA-ZnONPs; and (E) X-ray diffraction (XRD) pattern showing the characteristic reflections of the hexagonal wurtzite crystal structure of ZnO.

SEM analysis revealed predominantly spherical and hexagonal particle-like structures, with relatively uniform distribution and limited aggregation (Fig. 2A). EDX analysis detected zinc and oxygen as the major elemental constituents, with reported proportions of 44.87% and 55.13%, respectively (Fig. 2B). AFM analysis provided further information on the surface morphology of BA-ZnONPs. The two-dimensional topographical image showed the distribution of grain-like surface features (Fig. 2C), while the corresponding three-dimensional image revealed a non-uniform surface profile with prominent elevations (Fig. 2D). The positive surface skewness value (Ssk = 3.61) indicated a profile dominated by peaks, whereas the high kurtosis value (Sku = 26.1) reflected a pronounced distribution of sharp surface features.

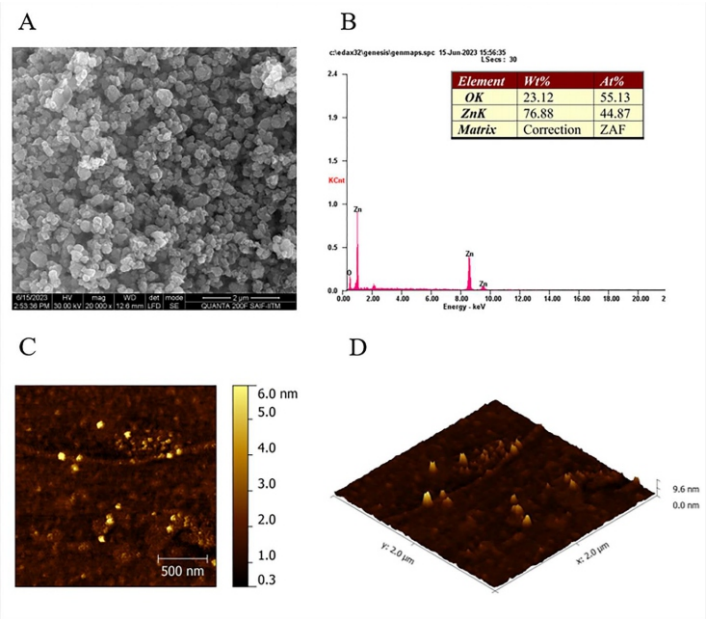

Fig. 2 Surface Morphology, Elemental Composition and Uniform Distribution of BA-ZnONPs. A.SEM B. EDX C. AFM 2D Topographical image BA-ZnONPs, D. AFM 3D surface morphology of BA-ZnONPs.

3.2. *In Vitro* Antidiabetic Activity of BA-ZnONPs

BA-ZnONPs exhibited concentration-dependent inhibition of α-amylase activity over the tested concentration range of 20–100 µg/mL (Fig. 3A). At 20 µg/mL, the nanoparticles produced 35.67 ± 2.32% inhibition, which increased progressively to 84.89 ± 2.46% at 100 µg/mL. This concentration-dependent response demonstrated the inhibitory potential of BA-ZnONPs against α-amylase, an enzyme involved in the hydrolysis of dietary starch. A pronounced inhibitory effect was also observed against α-glucosidase (Fig. 3B). Nonlinear regression analysis yielded an IC_{50} value of 43.34 µg/mL for BA-ZnONPs, compared with 90.14 µg/mL for the reference inhibitor acarbose. Thus, under the conditions of the present assay, BA-ZnONPs exhibited a lower IC_{50} value than acarbose, indicating greater inhibitory potency against α-glucosidase.

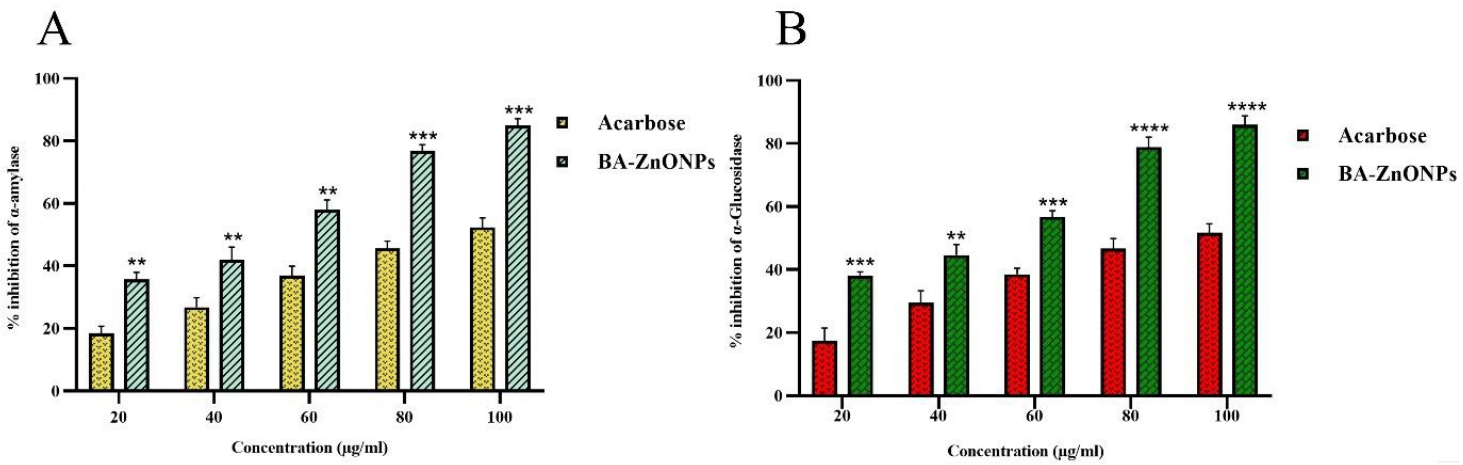

Fig. 3. Inhibitory effect of BA-ZnONPs on A. α-amylase and B. α-glucosidase activities.
Values are expressed as Mean ± SD (n = 3). Statistical significance was determined by one-way ANOVA, where **p < 0.01, ***p < 0.001, and ****p < 0.0001 compared to control.

3.3. Antihyperglycemic Activity of BAAE and BA-ZnONPs in STZ-Induced Diabetic Rats

3.3.1. Short-Term Effects of BAAE and BA-ZnONPs on Blood Glucose Levels and Glucose Tolerance

The short-term effects of BAAE and BA-ZnONPs on fasting blood glucose levels were evaluated over a 6-h period in STZ-induced diabetic rats (Table 1). The normal control group maintained relatively stable glucose concentrations throughout the observation period, ranging from 89 to 99 mg/dL. In contrast, the diabetic control group exhibited persistent hyperglycemia, with blood glucose increasing from 330 ± 7.32 mg/dL at baseline to 393 ± 9.98 mg/dL after 6 h. Treatment with BAAE and BA-ZnONPs produced time-dependent reductions in blood glucose levels. At the lower treatment doses, BAAE (250 mg/kg body weight) and BA-ZnONPs (25 mg/kg body weight) reduced blood glucose by 32.06% and 36.49%, respectively, after 6 h. At the higher doses, BAAE (500 mg/kg body weight) and BA-ZnONPs (50 mg/kg body weight) produced reductions of 53.57% and 59.23%, respectively. These findings indicate that both preparations reduced short-term hyperglycemia, with BA-ZnONPs producing a greater reduction at the corresponding lower and higher dose comparisons (Table 1).

Table 1: Short-Term effect of BA-ZnONPs on fasting blood glucose levels in STZ-induced experimental groups of rats

Groups	0hr	1hr	2hr	3hr	4hr	5hr	6hr
Normal control (NC)	93 ± 3.63	95 ± 2.97	98 ± 7.40	92 ± 2.45	89 ± 3.63	99 ± 4.43	94 ± 3.58
Diabetic control (STZ)	330 ± 7.32†	328 ± 9.55 ^{c}	347 ± 9.82 ^{c}	356 ± 7.92 ^{c}	376 ± 8.22 ^{c}	380 ± 9.01 ^{c}	393 ± 9.98 ^{c}
STZ+BAAE (250mg/kg b.w)	368 ± 8.22	357 ± 6.90	350 ± 7.16	343 ± 4.24	298 ± 9.06^{c} (19.02%)	285 ± 7.80^{c} (22.55%)	250 ± 8.32^{d} (32.06%)
STZ+BAAE (500mg/kg b.w)	364 ± 9.96	339 ± 9.90	321 ± 8.39	305 ± 8.51	267 ± 6.42^{c} (26.64%)	224 ± 8.41^{d} (38.46%)	169 ± 7.62^{d} (53.57%)
STZ+BA-ZnONPs (25mg/kg b.w)	370 ± 8.51	356 ± 8.74^{a}	342 ± 8.88 ^{b}	324 ± 7.92 ^{b}	279 ± 5.83 ^{c} (24.59%)	258 ± 6.66 ^{c} (30.27%)	235 ± 8.90 ^{d} (36.49%)
STZ+BA-ZnONPs (50mg/kg b.w)	363 ± 9.94	332 ± 5.83^{a}	310 ± 5.22 ^{b}	271 ± 9.57 ^{c}	250 ±4.86 ^{d} (31.13%)	209 ± 5.93 ^{d} (42.42%)	148 ± 9.94 ^{d} (59.23%)

† Indicates a statistically significant difference when compared with the normal control group.
Values are expressed as Mean ± SD (n = 6). ^{a}P < 0.05, ^{b} P < 0.01, ^{c} P < 0.001, ^{d} P < 0.0001. The percentage in parentheses indicates the percentage decrease in blood glucose compared to the 0-hour measurement.

The effects of BAAE and BA-ZnONPs on glucose tolerance were further evaluated using an oral glucose tolerance test (OGTT) (Fig. 4). Following glucose administration, the diabetic control group showed a marked increase in blood glucose, reaching 418 ± 4.73 mg/dL at 30 min and remaining elevated at 364 ± 2.76 mg/dL after 120 min. In comparison, treatment with BAAE and BA-ZnONPs attenuated the post-load increase in blood glucose and promoted a subsequent decline during the observation period.

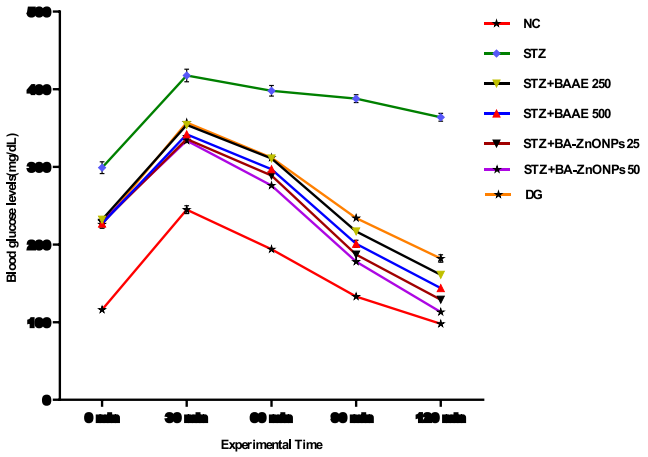

Fig. 4. The effect of BAAE and BA-ZnONPs on Oral Glucose Tolerance Test (OGTT) in diabetic rats induced by STZ. Results are reported as Mean ± SD (n = 6) and were determined by Statistical significance (p<0.05) by one-way ANOVA.

Among the nanoparticle-treated groups, BA-ZnONPs at 25 mg/kg body weight reduced blood glucose from 336 ± 3.90 mg/dL at 30 min to 129 ± 2.61 mg/dL at 120 min. The higher dose of BA-ZnONPs (50 mg/kg body weight) produced a further reduction, with glucose levels declining from 334 ± 2.61 mg/dL to 113 ± 1.67 mg/dL over the same interval. At 120 min, the glucose concentration in the 50 mg/kg BA-ZnONP-treated group was lower than that observed in the glibenclamide-treated group (182 ± 2.76 mg/dL). These findings demonstrate an improved glucose tolerance response following BA-ZnONP treatment, particularly at the higher dose (Fig. 4).

3.3.2. Long-Term Effects of BAAE and BA-ZnONPs on Glycemic Control

The effects of repeated administration of BAAE and BA-ZnONPs on fasting blood glucose levels were monitored over 42 days in STZ-induced diabetic rats (Table 2). The normal control group maintained relatively stable glucose concentrations, increasing from 89 ± 3.63 mg/dL at baseline to 102 ± 3.29 mg/dL on day 42. In contrast, the diabetic control group exhibited progressive hyperglycemia, with blood glucose increasing from 379 ± 1.79 mg/dL to 462 ± 1.55 mg/dL over the same period. Treatment with BAAE and BA-ZnONPs resulted in progressive reductions in fasting blood glucose levels. BAAE at 250 and 500 mg/kg body weight produced reductions of 64.72% and 75.78%, respectively, by day 42. BA-ZnONPs at 25 and 50 mg/kg body weight produced corresponding reductions of 69.49% and 79.07%, respectively. The reference drug glibenclamide (25 mg/kg body weight) reduced fasting blood glucose by 71.63% at the end of the experimental period.

Table 2: Effect of Long-Term Administration of BA-ZnONPs on Fasting Blood Glucose Levels in STZ-induced experimental Rats.

GROUPS	Blood Glucose Levels (mg/dL) During Long-Term Experimental Period						
	Initial	7th day	14th day	21st day	28th day	35th day	42nd day
Normal control **(NC)**	89 ± 3.63	94 ± 2.61	93 ± 3.90	102 ± 4.86	98 ± 2.76	101 ± 3.41	102 ± 3.29
Diabetic control **(STZ)**	379 ± 1.79 [a]	394 ± 1.67 [a]	403 ± 5.76 [a]	415 ± 2.90 [a]	421 ± 4.94 [a]	437 ± 4.24 [a]	462 ± 1.55 [a]
STZ+BAAE (250 mg/kg b.w)	407 ± 3.35	371 ± 3.74	259 ± 3.46	224 ± 3.85	196 ± 2.53	167 ± 2.61 **(58.96%)**	139 ± 3.29 **(64.72%)**
STZ+BAAE (500mg/kg b.w)	446 ± 4.69	382 ± 3.95	230 ± 3.22	197 ± 2.45	173 ± 4.05	144 ± 2.97 **(67.71%)**	108 ± 4.05 **(75.78%)**
STZ+BA-ZnONPs (25mg/kg b.w)	413 ± 1.55 [a]	375 ± 2.37 [b]	248 ± 2.45 [c]	211 ± 2.19 [c]	182 ± 1.10 [d]	152 ± 1.67 [d] **(63.19%)**	126 ± 1.41 [d] **(69.49%)**
STZ+BA-ZnONPs (50mg/kg b.w)	454 ± 1.26 [a]	347 ± 0.63 [b]	219 ± 3.85 [c]	190 ± 3.58 [c]	145 ± 3.41 [d]	104 ± 1.19 [d] **(77.09%)**	95 ± 3.16 [d] **(79.07%)**
(STZ+ Glibenclamide) (25mg /kg b.w)	423 ± 1.41 [a]	385 ± 1.10 [b]	251 ± 1.67 [c]	221 ± 3.88 [c]	196 ± 2.53 [d]	150 ± 2.45 [d] **(64.54%)**	120 ± 0.89 [d] **(71.63%)**

Results are presented as Mean ± SD (n = 6). [a] P < 0.01 compared with the baseline blood glucose level of the normal control group. [b] P < 0.05, [c] P < 0.001, and [d] P < 0.0001 denote statistically significant differences with the diabetic control group using one-way ANOVA followed by Tukey's post hoc test. Percentage reductions in blood glucose relative to the initial diabetic baseline values are mentioned in parentheses.

Among the tested treatments, BA-ZnONPs at 50 mg/kg body weight produced the greatest reduction in fasting blood glucose. In this group, glucose levels declined from 454 ± 1.26 mg/dL at baseline to 104 ± 1.19 mg/dL on day 35 and further to 95 ± 3.16 mg/dL on day 42. The reductions observed with BA-ZnONPs were therefore greater than those recorded with the corresponding BAAE treatment groups and the glibenclamide-treated group under the experimental conditions (Table 2).

3.3.3. Effects of BAAE and BA-ZnONPs on Body Weight and Hepatic Glucose Content

Changes in body weight during the experimental period are presented in Fig. 5A. The diabetic control group exhibited a marked reduction in body weight, with a net loss of approximately 55 g. In contrast, treatment with BAAE (500 mg/kg body weight) and BA-ZnONPs (50 mg/kg body weight) resulted in improvements in body weight, with reported net gains of approximately 45 and 50 g, respectively. These changes were statistically significant ($P < 0.05$) and indicated an improvement in body-weight maintenance in the treated diabetic animals. Hepatic glucose content was markedly elevated in the diabetic control group (5.89 ± 0.10 mg/g tissue) compared with the normal control group (2.94 ± 0.14 mg/g tissue), indicating altered hepatic glucose handling under diabetic conditions.

Treatment with BA-ZnONPs reduced hepatic glucose content in a dose-dependent manner. The 25 mg/kg body weight group showed a value of 3.12 ± 0.12 mg/g tissue, whereas the 50 mg/kg body weight group showed a further reduction to 2.86 ± 0.09 mg/g tissue, approaching the value observed in the normal control group. A reduction was also reported following treatment with BAAE and glibenclamide, with a value of 3.25 ± 0.21 mg/g tissue reported for the corresponding treatment comparison (Fig. 5B).

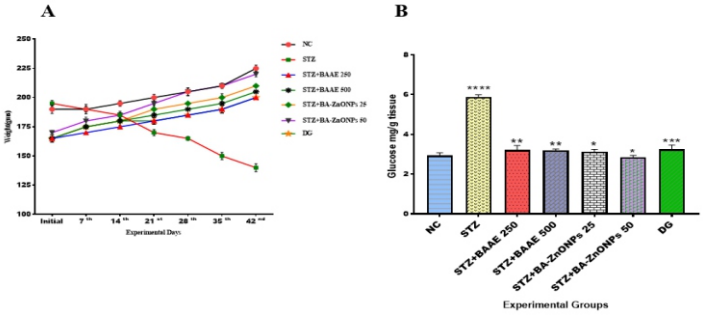

Fig. 5. Effect of BAAE and BA-ZnONPs on body weight and hepatic glucose levels of STZ- Induced diabetic rats.
Values are represented as Mean± SD (n = 6 statistical significance: ****p<0.0001, **p<0.005, and *p<0.05 when compared to the normal control.

3.3.4. Effects of BAAE and BA-ZnONPs on Glycogen Content and Carbohydrate-Metabolizing Enzymes

The effects of BAAE and BA-ZnONPs on hepatic and skeletal muscle glycogen contents are shown in Fig. 6. The normal control group exhibited hepatic and muscle glycogen levels of 25.93 ± 0.85 and 5.16 ± 0.44 mg/g tissue, respectively. In contrast, the diabetic control group showed reduced glycogen levels of 15.66 ± 0.46 mg/g tissue in the liver and 2.65 ± 0.34 mg/g tissue in skeletal muscle, indicating impaired glycogen storage under diabetic conditions. Treatment with BAAE (500 mg/kg body weight) increased hepatic glycogen content to 20.73 ± 0.32 mg/g tissue and muscle glycogen content to 4.05 ± 0.13 mg/g tissue. A greater restoration was observed following treatment with BA-ZnONPs (50 mg/kg body weight), which increased hepatic and muscle glycogen levels to 23.99 ± 0.38 and 4.92 ± 0.32 mg/g tissue, respectively. These values approached those observed in the normal control group, indicating improved glycogen restoration following BA-ZnONP administration (Fig. 6A, B).

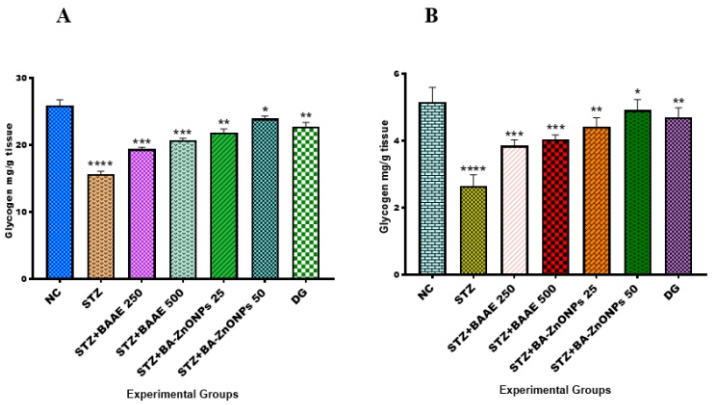

Figure 6. Effect of BAAE and BA-ZnONPs on Glycogen content in STZ-induced diabetic rats. A. Liver Glycogen B. Muscle Glycogen. Values are expressed as Mean ± SD (n = 6). Statistical significance was determined by one-way ANOVA, where ****p < 0.0001, ***p < 0.0005, **p < 0.005, *p < 0.05 compared to the normal control.

The activities of selected enzymes involved in carbohydrate metabolism were also evaluated (Fig. 7). The diabetic control group exhibited reduced activities of hexokinase and glucose-6-phosphate dehydrogenase (G6PDH) compared with the normal control group, indicating altered glucose utilization and associated metabolic activity. Treatment with BA-ZnONPs improved the activities of both enzymes. At 25 mg/kg body weight, the reported hexokinase and G6PDH activities were 0.186 ± 0.009 and 0.349 ± 0.016, respectively. These activities increased further to 0.212 ± 0.009 and 0.386 ± 0.012, respectively, following treatment with BA-ZnONPs at 50 mg/kg body weight. The glibenclamide-treated group also showed recovery of enzyme activities, with corresponding values of 0.204 ± 0.012 and 0.371 ± 0.018, respectively (Fig. 7A, B).

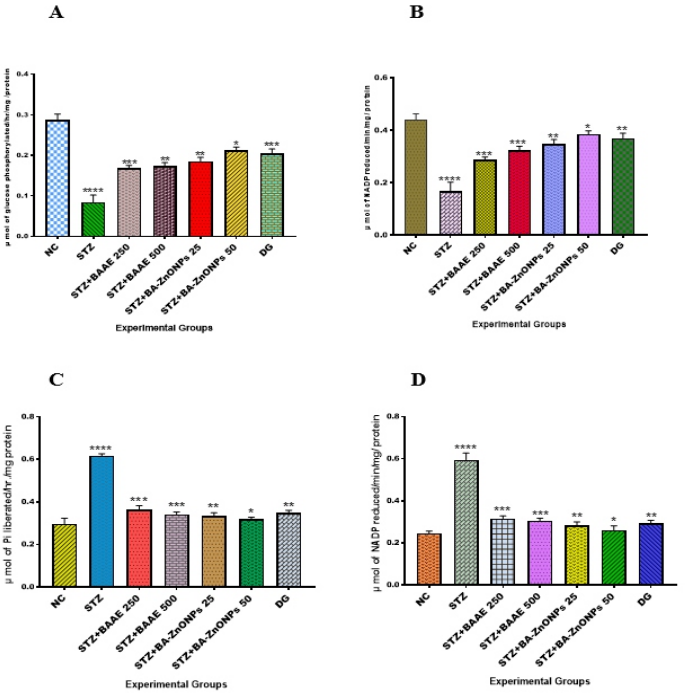

Fig. 7. Effect of BAAE and BA-ZnONPs on metabolic enzymes in STZ-induced diabetic rats. Glycolytic enzymes (A. Hexokinase, B. Glucose-6-phosphate dehydrogenase). Gluconeogenic enzymes. (C. fructose-1,6-bisphosphatase D. Glucose-6-Phosphotase)
Values are expressed as Mean ± SD (n = 6). Statistical significance was determined by one-way ANOVA, where ****p < 0.0001, ***p < 0.0005, **p < 0.005, *p < 0.05 compared to the normal control.

In contrast to the glycolytic enzymes, the activities of the gluconeogenic enzymes fructose-1,6-bisphosphatase and glucose-6-phosphatase were elevated in the diabetic control group. Fructose-1,6-bisphosphatase activity increased to 0.617 ± 0.010 µmol of Pi liberated/min/mg protein, compared with 0.298 ± 0.025 µmol of Pi liberated/min/mg protein in the normal control group. Glucose-6-phosphatase activity in the diabetic control group was reported as 0.596, compared with 0.246 ± 0.010 µmol of Pi liberated/min/mg protein in the normal control group. Treatment with BA-ZnONPs reduced the activities of both gluconeogenic enzymes in a dose-dependent manner. At 25 mg/kg body weight, fructose-1,6-bisphosphatase and glucose-6-phosphatase activities were 0.336 ± 0.013 and 0.285 ± 0.015 µmol of Pi liberated/min/mg protein, respectively. At 50 mg/kg body weight, the corresponding activities decreased further to 0.319 ± 0.009 and 0.262 ± 0.020 µmol of Pi liberated/min/mg protein, respectively (Fig. 7C, D). Collectively, these findings indicate that BA-ZnONPs treatment was associated with increased activities of selected glucose-utilization enzymes and reduced activities of key gluconeogenic enzymes in STZ-induced diabetic rats.

3.3.5. Histopathological Evaluation of Pancreatic Tissue

Histopathological examination revealed distinct differences in pancreatic architecture among the experimental groups (Fig. 8). The normal control group showed well-preserved islets of Langerhans and intact surrounding acinar cells. In contrast, the diabetic control group exhibited marked pathological alterations, including shrinkage and degeneration of the islets, cellular damage, necrotic changes, and congestion. Treatment with BAAE and BA-ZnONPs was associated with varying degrees of improvement in pancreatic tissue architecture. The BAAE-treated groups showed partial to improved preservation of the islets and surrounding acinar cells, with more evident structural improvement at 500 mg/kg body weight than at 250 mg/kg body weight. Similarly, the BA-ZnONP-treated groups exhibited relatively preserved islet architecture, with more pronounced improvement in the 50 mg/kg body weight group. The glibenclamide-treated group also showed improved islet structure and preservation of acinar cells compared with the diabetic control. Overall, the histological observations indicated improved preservation of pancreatic tissue architecture following treatment with BAAE and BA-ZnONPs, particularly at their respective higher doses (Fig. 8).

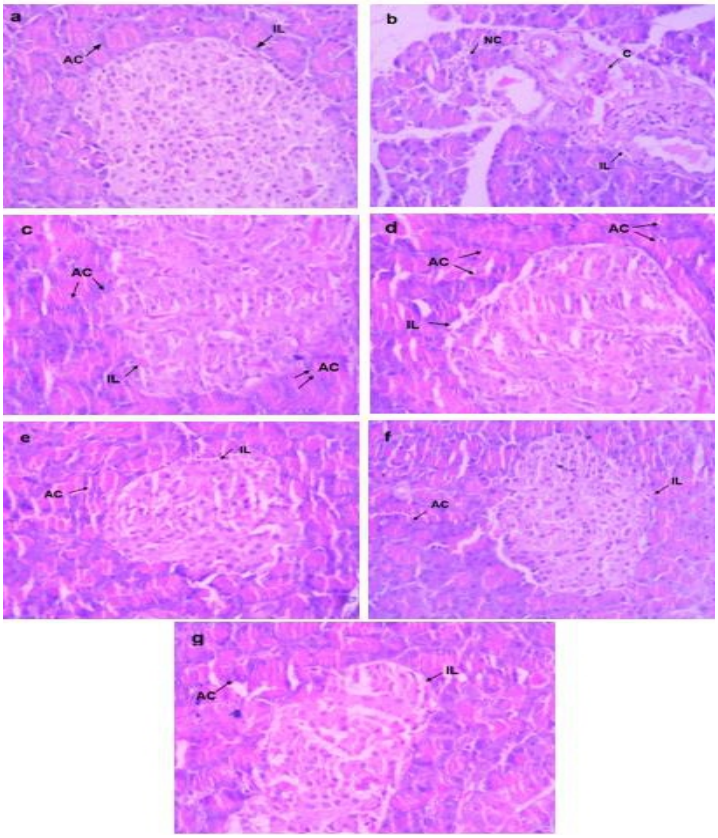

Fig. 8. Histopathological examination of pancreatic tissue from normal control, STZ-induced diabetic, and treatment groups. (a) Normal control showing normal islets of Langerhans and intact acinar cells; (b) diabetic control showing islet shrinkage and degeneration, necrotic changes, cellular damage, and congestion; (c) STZ + BAAE (250 mg/kg body weight) showing partial improvement in pancreatic architecture; (d) STZ + BAAE (500 mg/kg body weight) showing improved preservation of islets and acinar cells; (e) STZ + glibenclamide (25 mg/kg body weight) showing improved islet structure and preserved acinar cells; (f) STZ + BA-ZnONPs (25 mg/kg body weight) showing relatively preserved islet architecture and surrounding acinar cells; and (g) STZ + BA-ZnONPs (50 mg/kg body weight) showing marked preservation of islet architecture and pancreatic tissue organization. IL, islets of Langerhans; AC, acinar cells; NC, necrotic changes; C, congestion.

4. Discussion

The present study provides experimental evidence for the antidiabetic potential of BA-ZnONPs, based on their physicochemical characteristics, inhibitory effects on carbohydrate-hydrolyzing enzymes, and antihyperglycemic activity in STZ-induced diabetic rats. The findings indicate that phytomediated ZnO nanoparticle synthesis offers an approach for developing a plant-derived nanomaterial with biological activity relevant to glucose regulation. The observed effects were particularly evident in the enzyme inhibition assays, improvement in glucose tolerance, restoration of glycogen content, and modulation of carbohydrate-metabolizing enzyme activities. These findings provide a basis for further investigating the relationship between the physicochemical properties of BA-ZnONPs and their biological effects [28].

The physicochemical characterization supported the formation of ZnO nanoparticles using *B. alba* leaf extract. The distinct absorption maximum at 372 nm, together with the FTIR, XRD, SEM, EDX, and AFM findings, provided complementary evidence of nanoparticle formation and structural characteristics. The reported particle size of 1.4 nm and zeta potential of −38.2 mV further describe the physicochemical properties of the synthesized material [29,30]. The negative zeta potential suggests the presence of negatively charged surface-associated groups, potentially originating from plant-derived constituents, which may contribute to electrostatic stabilization of the nanoparticle suspension [31]. The changes in the FTIR absorption bands between BAAE and BA-ZnONPs also support the possible involvement of hydroxyl-, carbonyl-, and other oxygen-containing functional groups in nanoparticle formation and surface association. Previous studies have reported that the optical and electronic properties of ZnO nanomaterials, including their band-gap characteristics, are influenced by particle size, surface structure, and synthesis conditions [32,33]. However, the band-gap value of 3.33 eV should be considered a literature-based comparison rather than an experimentally established property of the present BA-ZnONPs preparation, unless supported by the corresponding optical calculations.

An important finding of the present investigation was the inhibitory activity of BA-ZnONPs against α-amylase and α-glucosidase, two enzymes involved in the digestion of dietary carbohydrates. Inhibition of these enzymes can reduce the rate of carbohydrate breakdown and subsequent glucose absorption, thereby providing a potential means of controlling postprandial hyperglycemia [34]. BA-ZnONPs produced concentration-dependent inhibition of α-amylase, with the percentage inhibition increasing from 35.67 ± 2.32% at 20 µg/mL to 84.89 ± 2.46% at 100 µg/mL. In the α-glucosidase assay, BA-ZnONPs exhibited an IC_{50} of 43.34 µg/mL, compared with 90.14 µg/mL for acarbose. The lower IC_{50} value indicates greater inhibitory potency of BA-ZnONPs under the conditions of this particular assay. Although this finding is encouraging, direct comparisons with the clinical effectiveness of acarbose cannot be made from an in vitro enzyme assay alone. Nevertheless, the results identify carbohydrate-hydrolyzing enzyme inhibition as one possible contributor to the antihyperglycemic activity of BA-ZnONPs.

The *in vivo* findings further supported the biological activity observed in the in vitro experiments. STZ administration produced sustained hyperglycemia in the experimental rats, whereas treatment with BAAE and BA-ZnONPs resulted in reductions in blood glucose levels. During the short-term assessment, BA-ZnONPs at 25 and 50 mg/kg body weight produced glucose reductions of 36.49% and 59.23%, respectively, after 6 h. The corresponding reductions with BAAE at 250 and 500 mg/kg body weight were 32.06% and 53.57%. Thus, BA-ZnONPs produced greater reductions than the aqueous extract at the respective tested doses. Notably, the higher nanoparticle dose produced a response comparable to, or greater than, that observed with the higher extract dose despite being administered at one-tenth of its mass dose. This difference suggests improved dose efficiency of the nanoparticle preparation under the experimental conditions, although it does not by itself establish enhanced bioavailability or a specific nanoparticle-mediated delivery mechanism. The improvement in glucose tolerance observed during the OGTT further supports the antihyperglycemic response, particularly at the 50 mg/kg dose of BA-ZnONPs [35,36].

The longer-term treatment findings provided additional evidence of the glucose-lowering activity of BA-ZnONPs. After 42 days, the reductions in fasting blood glucose were 64.72% and 75.78% for BAAE at 250 and 500 mg/kg body weight, respectively. In comparison, BA-ZnONPs at 25 and 50 mg/kg body weight produced reductions of 69.49% and 79.07%, respectively, while glibenclamide produced a reduction of 71.63%. The response observed with BA-ZnONPs at 50 mg/kg body weight was therefore greater than that recorded for the reference drug and the corresponding extract treatment in this experimental model. The improvement in body weight following treatment also contrasted with the marked weight loss observed in the diabetic control group. This finding may reflect improved metabolic status and reduced diabetes-associated tissue wasting. However, the underlying mechanisms responsible for the changes in body weight were not directly investigated in the present study.

Alterations in hepatic glucose content and tissue glycogen levels provided further insight into the effects of treatment on carbohydrate metabolism. The diabetic control group showed increased hepatic glucose content compared with the normal control, whereas BA-ZnONPs treatment reduced hepatic glucose levels towards the normal range. A similar pattern was observed for glycogen storage. The marked depletion of hepatic and skeletal muscle glycogen in diabetic control animals was accompanied by substantial restoration following treatment with BAAE and BA-ZnONPs. In particular, BA-ZnONPs at 50 mg/kg body weight increased hepatic glycogen content to 23.99 ± 0.38 mg/g tissue and muscle glycogen content to 4.92 ± 0.32 mg/g tissue, values approaching those of the normal control group. These observations suggest improved maintenance of tissue glycogen stores in treated animals. The findings are consistent with previous reports describing the involvement of zinc in glucose homeostasis, insulin-associated metabolic processes, and glycogen metabolism [37,38]. Earlier investigations have also reported beneficial effects of ZnO nanoparticles on glucose utilization and carbohydrate metabolism in experimental diabetic models [39,40].

The changes in carbohydrate-metabolizing enzyme activities provide additional support for the observed improvement in glucose regulation. The diabetic control group exhibited reduced activities of hexokinase and glucose-6-phosphate dehydrogenase (G6PDH), whereas treatment with BA-ZnONPs increased the activities of both enzymes. The improvement was more pronounced at 50 mg/kg body weight than at 25 mg/kg body weight. Hexokinase catalyzes the phosphorylation of glucose and is an important regulatory enzyme in glucose utilization, while G6PDH contributes to the pentose phosphate pathway and the generation of NADPH. Thus, the increased activities of these enzymes suggest an improvement in selected metabolic processes associated with glucose utilization. Conversely, the elevated activities of fructose-1,6-bisphosphatase and glucose-6-phosphatase observed in diabetic control animals were reduced following BA-ZnONPs treatment. Since these enzymes participate in hepatic gluconeogenesis, their reduced activities may indicate attenuation of gluconeogenic activity under the experimental conditions. The combined changes in glycolytic and gluconeogenic enzyme activities suggest a favourable shift in carbohydrate metabolism following treatment. These findings are consistent with previous reports describing the effects of ZnO-based nanomaterials on carbohydrate-metabolizing enzymes and glucose regulation in experimental diabetes [39,40].

Histopathological examination provided morphological evidence of treatment-associated improvement in pancreatic tissue. The diabetic control group displayed substantial alterations, including shrinkage and degeneration of the islets of Langerhans, cellular damage, necrotic changes, and congestion. In comparison, the BAAE- and BA-ZnONPs-treated groups exhibited varying degrees of preservation of islet architecture and surrounding acinar tissue. The most pronounced improvement was observed in the group treated with BA-ZnONPs at 50 mg/kg body weight. These observations are consistent with previous reports suggesting that plant-mediated ZnO nanoparticles may exert protective effects on pancreatic tissue in experimental models of diabetes [41]. However, the present histological findings demonstrate morphological preservation and improvement in tissue architecture rather than definitive β-cell regeneration. Confirmation of β-cell recovery would require additional investigations using specific markers, such as insulin immunostaining, together with quantitative assessment of β-cell mass and functional measurements of insulin secretion.

The biological effects of BAAE and BA-ZnONPs may be associated with the contribution of zinc to normal insulin biosynthesis, storage, and secretion, as well as its involvement in insulin-associated signalling and antioxidant defence mechanisms [42]. In addition, plant-derived constituents associated with the nanoparticle surface may contribute to the observed biological activity. The comparatively greater effects of BA-ZnONPs at lower administered doses suggest that nanoparticle formulation may influence the biological activity of the plant-derived preparation. Nevertheless, the individual contributions of zinc, the nanoparticle structure, and phytochemicals associated with the particle surface cannot be distinguished from the current experimental design. Previous studies on plant-mediated ZnO nanoparticles have also reported improvements in glycemic control, carbohydrate-metabolizing enzyme activities, glycogen content, and pancreatic histological features in experimental diabetic models [43].

The present findings are broadly consistent with these observations and extend the available evidence by evaluating *B. alba*-mediated ZnO nanoparticles alongside the corresponding aqueous extract.

Despite these encouraging results, certain limitations should be considered when interpreting the findings. The study did not include detailed molecular investigations of insulin signaling, glucose transporter expression, oxidative stress markers, inflammatory mediators, or the molecular pathways involved in pancreatic tissue preservation. Furthermore, the contribution of zinc ions and plant-derived surface-associated compounds to the observed biological effects was not independently established. The reported nanoparticle size also requires confirmation using complementary particle-sizing approaches to establish its accuracy. Additional studies involving mechanistic investigations, comprehensive toxicity assessment, pharmacokinetic evaluation, and longer-term treatment are therefore necessary to clarify the biological actions and safety profile of BA-ZnONPs [44,45]. Overall, the present findings identify *B. alba*-mediated ZnO nanoparticles as a promising candidate for further preclinical investigation of plant-based nanomaterials in diabetes-related research.

5. Conclusion

The present study demonstrates the promising antidiabetic potential of BAAE and BA-ZnONPs, as evidenced by their complementary in vitro and in vivo activities. BA-ZnONPs showed concentration-dependent inhibition of the carbohydrate-hydrolysing enzymes α-amylase and α-glucosidase. In streptozotocin-induced diabetic rats, treatment with BAAE and BA-ZnONPs improved glycaemic control and glucose tolerance, with the nanoparticle formulation at 50 mg/kg exhibiting the greatest reduction in fasting blood glucose among the tested treatments. These improvements were accompanied by favourable changes in body weight, hepatic and muscle glycogen content, carbohydrate-metabolising enzyme activities, and pancreatic histological architecture. The observed effects suggest that the antidiabetic activity of BA-ZnONPs may involve the combined contributions of zinc oxide and *B. alba*-derived phytochemicals, potentially influenced by the physicochemical properties of the nanoscale formulation. However, the relative contributions of zinc, plant-derived constituents, and nanoparticle-specific effects remain to be established. Overall, BA-ZnONPs represent a promising plant-mediated nanomaterial for further investigation in diabetes management. Detailed mechanistic studies, together with comprehensive dose-dependent toxicity, pharmacokinetic, and long-term safety assessments, are necessary before their therapeutic potential can be translated into clinical applications.

Declaration of competing interests

The authors declare that they have no known competing financial interests or personal relationships that could have appeared to influence the work reported in this paper.

CRediT authorship contribution statement

Swathi Badabagni: Methodology, Research, Data curation, Formal analysis, Writing – original draft. Palempalli Uma Maheswari Devi: Conceptualization, Supervision, Validation, Funding acquisition, Project administration, Writing – review & editing. O Vijaya Sarathi Reddy: Conceptualization, Supervision, Validation, Writing – review & editing. Balaji Meriga: Methodology, Research, Data curation, Formal analysis, Writing – original draft.

Funding

This research did not receive any specific grant from funding agencies in the public, commercial, or not-for-profit sectors.

References

1. Alam S, Hasan MK, Neaz S, Hussain N, Hossain MF, Rahman T. Diabetes Mellitus: insights from epidemiology, biochemistry, risk factors, diagnosis, complications and comprehensive management. Diabetology. 2021;2(2):36-50. doi: https://doi.org/10.3390/diabetology2020004
2. Tavakoli M, Klingelhöfer D, Fadavi H, Groneberg DA. The landscape of global research on diabetic neuropathy. Front. Endocrinol. 2023;14:1220896. doi: https://doi.org/10.3389/fendo.2023.1220896
3. Kazi S. Use of traditional plants in diabetes mellitus: a review. Int. J. Pharm. 2014;4(4):283-289.
4. Zargar AH, Shah NA, Masoodi SR, Laway BA, Dar FA, Khan AK, et al. 2002. Copper, zinc and magnesium level in type-1 diabetes mellitus. Saudi Med. J. 2002;23(5):539-542. PMID:12070576.
5. Chausmer AB. Zinc, insulin and diabetes. J. Am. Coll. Nutr. 1998;17(2):109-115. doi: https://doi.org/10.1080/07315724.1998.10718735.
6. Ceriello A, Prattichizzo F, Phillip M, Hirsch IB, Mathieu C, Battelino T. Glycaemic management in diabetes: old and new approaches. Lancet Diabetes Endocrinol. 2022;10(1):75-84. doi: https://doi.org/10.1016/S2213-8587(21)00245-X
7. Halayal RY, Bagewadi ZK, Khan TY, Shamsudeen SM. Investigating compounds from Basella alba for their antioxidant, anti-inflammatory, and anticancer properties through in vitro and network pharmacology, molecular simulation approach. Green Chem. Lett. Rev. 2025;18(1):2481945. doi: https://doi.org/10.1080/17518253.2025.2481945
8. Sheik A, Kim E, Adepelly U, Alhammadi M, Huh YS. Antioxidant and antiproliferative activity of Basella alba against colorectal cancer. Saudi J. Biol. Sci. 2023;30(4):103609. doi: https://doi.org/10.1016/j.sjbs.2023.103609
9. Sutor-Swiezy K, Górska R, Kumorkiewicz-Jamro A, Dziedzic E, Bieniasz M, Mielczarek P, et al. Basella alba L. (Malabar Spinach) as an abundant source of betacyanins: identification, stability, and bioactivity studies on natural and processed fruit pigments. J. Agric. Food Chem. 2024;72(6):2943-2962. doi: https://doi.org/10.1021/acs.jafc.3c06225.
10. Khattak U, Jan S, Ullah R, Haq TU, Khan MN, Iqbal M, et al. Green synthesis and physical characterization of zinc oxide nanoparticles (ZnO NPs) derived from the methanol extract of Euphorbia dracunculoides Lam. (Euphorbiaceae) with enhanced biosafe applications. Green Process. Synth. 2024;13(1):20240119. doi: https://doi.org/10.1515/gps-2024-0119.
11. Parvin N, Aslam M, Joo SW, Mandal TK. Nano-Phytomedicine: Harnessing Plant-Derived Phytochemicals in Nanocarriers for Targeted Human Health Applications. Molecules. 2025;30(15):3177. doi: https://doi.org/10.3390/molecules30153177.
12. Agarwal H, Kumar SV, Rajeshkumar S. A review on green synthesis of zinc oxide nanoparticles- an eco-friendly approach. Resour. Effic. Technol. 2017;3(4):406-413. doi: https://doi.org/10.1016/j.reffit.2017.03.002.
13. Jiang J, Pi J, Cai J. The advancing of zinc oxide nanoparticles for biomedical applications. Bioinorg. Chem. Appl. 2018;2018:1062562. doi: https://doi.org/10.1155/2018/1062562.
14. Khan I, Saeed K, Khan I. Nanoparticles: properties, applications and toxicities. Arab. J. Chem. 2019;12(7):908-931. doi: https://doi.org/10.1016/j.arabjc.2017.05.011.

15. Ukperoro JU, Offiah N, Idris T, Awogoke D. Antioxidant effect of zinc, selenium and their combination on the liver and kidney of alloxan-induced diabetes in rats. Mediterr. J. Nutr. Metab. 2010;3(1):25-30. doi: https://doi.org/10.3233/s12349-009-0069-9.
16. Vinotha V, Iswarya A, Thaya R, Govindarajan M, Alharbi NS, Kadaikunnan S, et al. Synthesis of ZnO nanoparticles using insulin-rich leaf extract: Anti-diabetic, antibiofilm and anti-oxidant properties. J. Photochem. Photobiol. B: Biol. 2019;197:111541. doi: https://doi.org/10.1016/j.jphotobiol.2019.111541.
17. Gnanasangeetha D, Sarala Thambavani D. One Pot Synthesis of Zinc Oxide Nanoparticles via Chemical and Green Method. Res. J. Mater. Sci. International Science Congress Association 2013;1(7):1-8.
18. Bernfeld P. Amylases α and β. Methods. Enzymol. 1955;1:149-158. doi: https://doi.org/10.1016/0076-68791(55)01021-5.
19. Kim YM, Jeong YK, Wang MH, Lee WY, Rhee HI. Inhibitory effect of pine extract on α-glucosidase activity and postprandial hyperglycemia. Nutrition. 2005;21(6):756-761. doi: https://doi.org/10.1016/j.nut.2004.10.014.
20. Kifayatullah M, Mustafa MS, Sengupta P, Sarker MMR, Das A, Das SK. Evaluation of the acute and sub-acute toxicity of the ethanolic extract of Pericampylus glaucus (Lam.) Merr. In BALB/c mice. J. Acute. Dis. 2015;4(4):309-315. doi: https://doi.org/10.1016/j.joad.2015.06.010.
21. Vani M, Devi PUM. Seagrass in the control of hyperglycemic and hyperlipidemic states of streptozotocin-induced diabetic rats. Pharmacogn J. 2020;12(6 Suppl):1716-1721. doi: https://doi.org/10.5530/pj.2020.12.232.
22. Akbarzadeh A, Norouzian D, Mehrabi MR, Jamshidi SH, Farhangi A, Allah Verdi A, et al. Induction of diabetes by streptozotocin in rats. Indian j Clin Biochem. 2007;22(2):60-64. doi: https://doi.org/10.1007/BF02913315.
23. Nelson N. A photometric adaptation of the Somogyi method for the determination of glucose. J. Biol. Chem. 1944;153(2):375-380. doi: https://doi.org/10.1016/S0021-9258(18)71980-7.
24. Somogyi M. Notes on sugar determination. J. Biol. Chem. 1952;195(1):19-23. doi: https://doi.org/10.1016/S0021-9258(19)50870-5.
25. Gao H, Leary JA. Multiplex inhibitor screening and kinetic constant determinations for yeast hexokinase using mass spectrometry-based assays. J. Am. Soc. Mass Spectrom. 2003;14(2):173-181. doi: https://doi.org/10.1016/S1044-0305(02)00867-X
26. Minucci A, Moradkhani K, Hwang MJ, Zuppi C, Giardina B, Capoluongo E. Glucose-6-phosphate dehydrogenase laboratory assay: how when, and why? IUBMB Life. 2009;61(1):27-34. doi: https://doi.org/10.1002/iub.137.
27. Fiske CH, Subbarow Y. The colorimetric determination of phosphorus. J. Biol. Chem. 1925;66(2):375-400. doi: https://doi.org/10.1016/S0021-9258(18)84756-1.
28. Assad N, Abbas A, Rehman MFU, Naeem-ul-Hassan M. Photo-catalytic and biological applications of phyto-functionalized zinc oxide nanoparticles synthesized using a polar extract of Equisetum diffusum D. RSC Adv. 2024;14(31):22344-22358. doi:10.1039/D4RA03573.
29. Carroll NV, Longley RW, Roe J H. The determination of glycogen in liver and muscle by use of anthrone reagent. J. Biol. Chem. 1956;220(2):583-593. doi: https://doi.org/10.1016/S0021-9258(18)65284-6.
30. Özgür Ü, Alivov YI, Liu C, Teke A, Reshchikov MA, Doğan S, et al. A comprehensive review of ZnO materials and devices. J. Appl. Phys. 2005;98(4):041301. doi: https://doi.org/10.1063/1.1992666.
31. Klingshirn C. ZnO: From basics towards applications. Phys. Status Solidi B. 2007;244(9):3027-3073. doi: https://doi.org/10.1002/pssb.200743072.
32. Abid HK, Siddique AB, Abbas A, Shaheen MA, Ali A, Fatima M, et al. Biogenic synthesis of ZnO NPs, CuO NPs, and ZnO/CuO nanocomposites for facile degradation of organic pollutants and biomedical applications. Nanoscale Adv. 2025;7(19):6145-6157. doi:10.1039/D5NA00583C.
33. Aqeela S, Siddique AB, Abbas A, Majid A, Sikandar B, Shaheen MA, et al. Antioxidant potential and increased photocatalytic efficiency of gallic acid-capped ZnO and NiO NPs for azo dye degradation: effect of heterojunction coupling and machine learning-assisted modeling. Nanoscale Adv. 2026;8(1):224-239. doi:10.1039/D5NA00827A.
34. Yassin MT, Al-Askar AA, Maniah K, Alotibi FO. Green Synthesis of Zinc Oxide Nanocrystals Utilizing Origanum majorana Leaf Extract and Their Synergistic Patterns with Colistin against Multidrug-Resistant Bacterial Strains. Crystals. 2022;12(11):1513. doi: https://doi.org/10.3390/cryst12111513.
35. Szkudelski T. The mechanism of alloxan and streptozotocin action in B cells of the rat pancreas. Physiol. Res. 2001;50(6):537-546. doi: https://doi.org/10.33549/physiolres.930111.
36. King AJF. The use of animal models in diabetes research. Br. J. Pharmacol. 2012;166(3):877-894. doi: https://doi.org/10.1111/j.1476-5381.2012.01911.x.
37. Alkaladi A, Abdelazim AM, Afifi M. Antidiabetic activity of zinc oxide and silver nanoparticles on streptozotocin-induced diabetic rats. Int. J. Mol. Sci. 2014;15(2):2015-2023. doi: https://doi.org/10.3390/ijms15022015.
38. Umrani RD, Paknikar KM. Zinc oxide nanoparticles show antidiabetic activity in streptozotocin-induced type 1 and 2 diabetic rats. Nanomedicine (Lond). 2014;9(1):89-104. doi: https://doi.org/10.2217/nnm.12.205.
39. Siddiqui SA, Or Rashid MM, Uddin MG, Robel FN, Hossain MS, Haque MA, et al. Biological efficacy of zinc oxide nanoparticles against diabetes: a preliminary study conducted in mice. Biosci. Rep. 2020;40(4):BSR20193972. doi: https://doi.org/10.1042/BSR20193972.
40. Al Sulimani MM, El Hamidy SM, Shaikh Omar AM. The possible antihyperglycemic effects of zinc oxide nanoparticles on diabetes induced by streptozotocin in male rats. Curr. Sci. Int. 2024;13(1):1-32. doi: https://doi.org/10.36632/csi/2024.13.1.5.
41. El-Gharbawy RM, Emara AM, Abu-Risha SE. Zinc oxide nanoparticles and a standard antidiabetic drug restore the function and structure of beta cells in type-2 diabetes. Biomed. Pharmacother. 2016;84:810-820. doi: https://doi.org/10.1016/j.biopha.2016.09.068.
42. Ghaffar S, Abbas A, Naeem-ul-Hassan M, Assad N, Sher M, Ullah S, Alhazmi HA, Najmi A, Zoghebi K, Al Bratty M, et al. Improved Photocatalytic and Antioxidant Activity of Olive Fruit Extract-Mediated ZnO Nanoparticles. Antioxidants. 2023;12(6):1201. https://doi.org/10.3390/antiox12061201
43. Ullah S, Shaban M, Siddique AB, Zulfiqar A, Lali NS, Naeem-ul-Hassan M, et al. Greenly synthesized zinc oxide nanoparticles: an efficient, cost-effective catalyst for dehydrogenation of formic acid and with improved antioxidant and phyto-toxic properties. J Environ Chem Eng. 2024;12(5):113350. doi:10.1016/j.jece.2024.113350.
44. John AD, Ramasamy R, Natarajan S, Sadiq AM, Rathinam A. Protective role of biosynthesised zinc oxide nanoparticles on pancreatic beta cells: an in vitro and in vivo approach. IET Nanobiotechnol. 2020;14(9):756-760. doi: https://doi.org/10.1049/iet-nbt.2020.0084.
45. Gadoa ZA, Moustafa EM, Ahmed OM, et al. Zinc oxide nanoparticles and synthesized pyrazolopyrimidine alleviate streptozotocin-induced diabetes in rats. ACS Omega. 2022;7:38795-38805. doi: https://doi.org/10.1021/acsomega.2c05638.